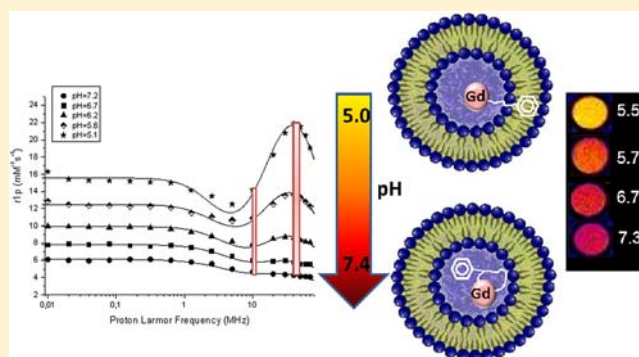


## Relaxometric Investigations and MRI Evaluation of a Liposome-Loaded pH-Responsive Gadolinium(III) Complex

E. Gianolio,<sup>†</sup> S. Porto,<sup>†</sup> R. Napolitano,<sup>†</sup> S. Baroni,<sup>‡</sup> G.B. Giovenzana,<sup>§</sup> and S. Aime<sup>\*,†</sup><sup>†</sup>Department of Chemistry & Molecular Imaging Center, University of Torino, Via Nizza 52, Torino, Italy<sup>‡</sup>Invento SRL, University of Torino, Via Nizza 52, Torino, Italy<sup>§</sup>DiSCAFF, Università del Piemonte Orientale "A. Avogadro", Via Bovio 6, 28100 Novara, Italy

## Supporting Information

**ABSTRACT:** Accurate measurement of the tissue pH in vivo by MRI may be of clinical value for both diagnosis and selection/monitoring of therapy. To act as pH reporters, MRI contrast agents have to provide responsiveness to pH that does not require prior knowledge of the actual concentration of the contrast agent. This work deals with the use of a paramagnetic gadolinium(III) complex, loaded into liposomes, whose relaxometric properties are affected by the pH of the medium. In this system, the amphiphilic metal complex, which contains a moiety whose protonation changes the coordination properties of the metal chelate, experiences a different intraliposomal distribution depending on the pH conditions. The pH of the solution can be unambiguously identified by exploiting the peculiar characteristics of the resulting NMRD profiles, and a ratiometric pH-responsive method has been set up by comparing the relaxation enhancement at different magnetic field strengths.



## INTRODUCTION

Mapping the pH at the high spatial resolution of magnetic resonance (MR) images is a task of considerable interest because the pH appears to be an important biomarker in the diagnostic assessment of diseases such as stroke, tumor, and infections. To this purpose, several approaches have been undertaken.

(1) Use of paramagnetic metal complexes whose ability to enhance the proton relaxation rate (commonly called relaxivity) of their solution is pH-dependent. The most straightforward approach relies on the design of chelating moieties that are involved in a protonation/deprotonation step that yields to changes in the denticity of the ligand. In turn, this results in changes in the number of water molecules coordinated to the paramagnetic metal ion. Some years ago, it was reported that inclusion of a sulfonamide moiety in a macrocyclic ligand (Gd-DO3Asa) can yield a gadolinium(III) chelate whose relaxivity is pH-dependent as a consequence of a change in the hydration state ( $q$ ).<sup>1</sup> Because the relaxivity of a paramagnetic metal complex scales up with hydration of the metal ion, the relaxivity of these types of complexes is dependent on the pH in a range of values characteristic of the protonation/deprotonation step. Alternatively, it has been shown that a pH-dependent relaxivity can be obtained if the mobility of the paramagnetic complex is affected by the pH of the solution.<sup>2</sup> Other approaches dealing with pH-dependent relaxivity changes of paramagnetic metal complexes were based on changes in the second coordination sphere.<sup>3</sup> All of these approaches failed the in vivo translation because of the need to know the local concentration of the

paramagnetic agent in order to pursue transformation of the observed relaxation rates into relaxivity data. Without this information, the detected changes in  $T_1$  could be ascribed either to changes in the relaxivity or to changes in the local concentration of the paramagnetic metal complex.

Routes have been proposed to overcome this drawback. For example, through the setup of a poly( $\beta$ -cyclodextrin)/<sup>19</sup>F/Gd-L adduct in which the <sup>19</sup>F-containing moiety reports on the concentration of the MR-responsive gadolinium complex<sup>4</sup> or, more recently, of a dual MR imaging (MRI)/positron emission tomography (PET) pH-responsive system, reported by Caravan et al.,<sup>5</sup> in which the local quantitation of the dual imaging agent is provided by the PET moiety. A related MRI/SPECT agent for mapping the pH has recently been reported in which the SPECT-active moiety acts as a reporter of the concentration, thus allowing transformation of the observed <sup>1</sup>H relaxation rates into relaxivities to recover the information relative to the pH determination.<sup>6</sup>

(2) Use of chemical exchange saturation transfer (CEST) agents containing two pools of exchangeable protons in the same molecule whose exchange rate with the "bulk" water protons is catalyzed to a different extent by the solution pH.<sup>7</sup> The comparison between the CEST effect generated by the selective irradiation of each pool of exchangeable protons provides a method for assessing the solution pH that is independent of the

Received: February 28, 2012

Published: June 20, 2012

knowledge of the actual concentration of the CEST agent. For in vivo translation, the method suffers from a limited sensitivity because millimolar concentrations of the exchangeable proton pools are required.

(3) Use of a hyperpolarized  $\text{H}^{13}\text{CO}_3^-/^{13}\text{CO}_2$  mixture.<sup>8</sup> Because the ratio between the two species is pH-dependent, the detection of their ratio in a spectroscopic MR image allows pH assessment. The method is not of general applicability because only a very few laboratories are equipped with a very expensive polarizer. Other experimental issues (e.g., line width of  $^{13}\text{CO}_2$ ) make unlike the translation of this method to the clinical practice.

(4) pH-sensitive liposomes have also been reported.<sup>9</sup> Liposomes are vesicles consisting of an aqueous inner cavity surrounded by a double layer of phospholipids analogous to the structure of cellular membranes. The permeability of the phospholipid bilayers to water molecules can be well controlled by modulating the phospholipid composition as well as with the addition of cholesterol. pH-sensitive liposomes consist of systems containing a paramagnetic metal complex in the inner aqueous cavity, whereas their membrane is designed to give low permeability to water molecules at neutral pH. These liposomes are essentially MRI-silent at neutral pH, with a marked increase of the water proton relaxation rates at acidic pH, where protonation of a substituent of the lipidic components leads to a change in the lipid organization. This change corresponds to the release of the paramagnetic payload. Thus, as far as its use for monitoring the pH is concerned, such a system does not appear to be a suitable one because the lack of reversibility is clearly an undesired property for this application.

Thus, a reliable, highly sensitive method for pH mapping in MRI that acts independently from the knowledge of the actual concentration of the pH-responsive probe appears definitively useful and timely for the development of novel diagnostic procedures based on in vivo pH mapping.

Herein we report results aimed at developing a new ratiometric method based on inclusion of the Gd-DO3Asa complex in liposomes. The amphiphilic metal complex, containing a moiety whose protonation changes the coordination properties of the metal chelate, experiences a different intraliposomal distribution depending on the pH conditions. The ratiometric method consists of measuring the pH dependence of the ratio between the longitudinal paramagnetic contribution to the water proton relaxation rates ( $R_{1p}$ ) at two different magnetic fields, thus removing the concentration dependence of the MR signal.

## EXPERIMENTAL SECTION

**Liposome Preparation.** Large unilamellar vesicles (LUVs) were prepared by following the lipidic thin-film hydration method. Briefly, the lipids (about 30 mg/mL in total including phospholipids and cholesterol) were dissolved in chloroform, and the organic solution was slowly evaporated to remove the solvent until a thin film was formed. The film was then hydrated at 55 °C with neutral aqueous solutions containing different concentrations (4, 8, and 32 mM) of the pH-sensitive Gd-DO3Asa complex, 150 mM NaCl, and 2 mM phosphate buffer. The resulting suspension of multilamellar vesicles was extruded (Lipex extruder, Northern Lipids Inc., Burnaby, British Columbia, Canada) two times through polycarbonate filters of 400 nm and four times through 200 nm filters. The final suspension of LUV was purified from the nonencapsulated gadolinium complex by exhaustive dialysis carried out at 25 °C against an iso-osmolar NaCl solution. The following phospholipidic membrane formulations have been used: (A) 70% POPC, 25% cholesterol, 5% PEG-2000-methoxy; (B) 35% POPC, 35% DPPC, 25% cholesterol, 5% PEG-2000-methoxy.

The pH values of the liposomes' suspensions were changed (in the pH range 5–7.4) by the slow addition of small amounts of concentrated HCl and NaOH solutions.

**Liposome Size Measurement.** The vesicle dispersions were diluted 100 times and investigated by DLS (Zetasizer NanoZS, Malvern, U.K.) in order to assess the mean hydrodynamic diameter and the polydispersity of the system. The polydispersity indices (PDIs) for all liposomes used in this work were between 0.1 and 0.2.

**Relaxometric Characterization.** The longitudinal water proton relaxation rate as a function of the pH was measured by using a Stellar Spinmaster (Stelar, Mede, Pavia, Italy) spectrometer operating at 20 MHz, by means of the standard inversion–recovery technique. The temperature was controlled with a Stelar VTC-91 airflow heater equipped with a copper–constantan thermocouple (uncertainty 0.1 °C). The proton  $1/T_1$  NMRD profiles were measured over a continuum of magnetic field strength from 0.00024 to 0.47 T (corresponding to 0.01–20 MHz proton Larmor frequencies) on a Stellar field-cycling relaxometer. The relaxometer works under complete computer control with an absolute uncertainty in  $1/T_1$  of 1%. Data points from 0.47 T (20 MHz) to 1.7 T (70 MHz) were collected on a Stellar Spinmaster spectrometer working at variable field. The concentration of the gadolinium complex solutions, for relaxometric characterization, was determined by mineralizing a given quantity of the sample solution by the addition of 37% HCl at 120 °C overnight. From measurement of the observed relaxation rate ( $R_{1\text{obs}}$ ) of the acidic solution and knowing the relaxivity ( $r_{1p}$ ) of  $\text{Gd}^{\text{III}}$  aquaion in acidic conditions ( $13.5 \text{ mM}^{-1} \text{ s}^{-1}$ ), it was possible to calculate the exact gadolinium(III) concentration (this method was calibrated using standard ICP solutions, and the accuracy was determined to be <1%).

**MRI Investigations.** MR images of a phantom consisting of five tubes filled with liposome dispersions at different values of the gadolinium(III) concentration and pH were measured on a Aspect MRI scanner operating at 1 T and on a Esaote clinical scanner operating at 0.2 T.  $T_1$ -weighted images were acquired under the same conditions for the two instruments by applying a routine spin–echo sequence with TR/TE/NEX = 150/18/10, FOV  $3 \times 3 \text{ cm}^2$ , and 1 slice 2 mm.  $T_1$  values were measured using an inversion–recovery spin–echo sequence (TE = 8 ms, 10 variable TR ranging from 40 to 4000 ms, NEX = 7, FOV =  $3 \times 3 \text{ cm}^2$ , 1 slice 2 mm).

## RESULTS AND DISCUSSION

**Relaxometric Analysis of Liposomes Containing the Gd-DO3Asa Complex.** It is well-known that amphiphilic metal complexes can be incorporated in the liposome's membrane either when they are one of the components of the lipid film or when they are dissolved in the hydration solution.

When the amphiphilic complex contains a  $\text{Gd}^{\text{III}}$  ion, its incorporation into the liposome's membrane is witnessed by the occurrence of a relaxation enhancement of water protons, which is dependent on the applied magnetic field and characterized by a typical “hump” at 35–40 MHz in the NMRD profile.<sup>10</sup>

In this work, liposomes loaded with the amphiphilic Gd-DO3A derivative (Gd-DO3Asa) represented in Figure 1 have been used. This complex was reported some years ago to display a relaxivity dependence on the pH of its solutions because the sulfonamide moiety, having  $\text{p}K_a = 6.7$ , enters the metal coordination cage only at relatively high pH values.<sup>1</sup> Therefore,

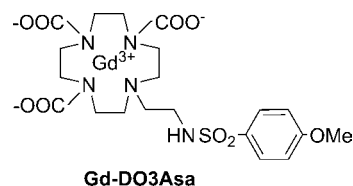
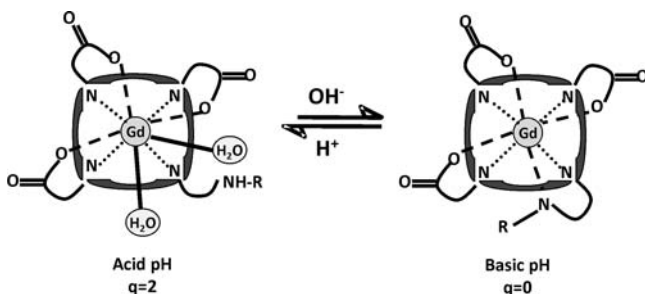


Figure 1. Structural formula of the Gd-DO3Asa complex.

Gd-DO3Asa displays high relaxivity at acidic pH values when the gadolinium(III) coordination sphere may host up to two water molecules and low relaxivity at basic pH values when the entering of the deprotonated sulfonamide moiety into the coordination scheme causes exclusion of any directly coordinated water molecule (Scheme 1).

**Scheme 1. Graphical Representation of the pH-Dependent Coordination Scheme of the Gd-DO3Asa Complex**



Liposomes endowed with different membrane water permeabilities [namely, for liposome A, 70% POPC, 25% Chol, 5% PEG-2000-methoxy (higher permeability), and for liposome B, 35% POPC, 35% DPPC, 25% Chol, and 5% PEG-2000-methoxy (lower permeability)] were loaded with the Gd-DO3Asa complex through hydration of the lipidic film with solutions of the gadolinium complex at 4 mM concentration and pH 7.

Measurements of their relaxivity as a function of the pH at 20 MHz and 298 K (Figure 2a) indicate that, upon entrapment in the liposomes, the relaxivity of Gd-DO3Asa maintains the pH-dependent behavior shown by the free complex. Moreover, incorporation of the gadolinium complex into the liposome membrane leads to an even steeper change in the relaxivity in the pH range 5–7.5. The liposomes' integrity as a function of the pH variation was assessed by dynamic light scattering (DLS), and diameters in the range 120–140 nm were invariantly determined over the entire investigated pH range, indicating that the pH does not cause fusion of liposomes, as reported for systems designed to release their payload at acidic pH values.

A deeper understanding of the processes has been gained through the acquisition and analysis of NMRD profiles of the two liposomes in the pH range 5–7.4 (Figure 3 and Table 1). For comparison, the NMRD profile of the Gd-DO3Asa complex in water at pH 5 was also recorded (Figure 2b, black squares).

The observed behavior could be, at least in part, accounted for by a different distribution of the gadolinium complex between the internal liposomal aqueous cavity and the phospholipidic membrane. NMRD data were then fitted by using a theoretical model based on the classical Solomon–Bloembergen–Morgan equations<sup>11</sup> modified to take into account the different distributions of the gadolinium responsive agent in the liposomal system and the water exchange rate across the liposome's membrane (Supporting Information). Such a model includes a distribution factor ( $f$ ) that accounts for the fraction of membrane-intercalated gadolinium complexes with respect to the complexes simply encapsulated in the internal cavity and a value ( $P_w$ ) for the water permeability of the liposome's membrane. By using this model, two distinct sets of relaxometric parameters ( $\tau_R$ ,  $\tau_M$ ,  $\Delta^2$ ,  $\tau_V$ , and  $q$ ) have been considered for encapsulated and membrane-intercalated gadolinium complexes, respectively.

Fitting of the experimental data for the free gadolinium complex in aqueous solution (Figure 2b) and for the gadolinium complex in the liposome, at different pH values, leads to determination of a quite solid set of parameters. In fact, when data measured under the same pH conditions are considered, the obtained parameters for the main determinants of the observed relaxivity for the encapsulated fraction of the gadolinium complex are similar to those determined for the free complex. With regards to the parameters relative to the membrane-intercalated fraction, the following conclusions may be drawn: (i) parameters governing the electronic relaxation times ( $\Delta^2$  and  $\tau_V$ ) are in the range of reported values for similar systems,<sup>12</sup> (ii) the reorientational correlation time ( $\tau_R$ ) is considerably increased with respect to the value found for the free complex, as expected on the basis of the slower motion of the liposomal vesicle; (iii) the exchange lifetime of the coordinated water molecule ( $\tau_M$ ) is

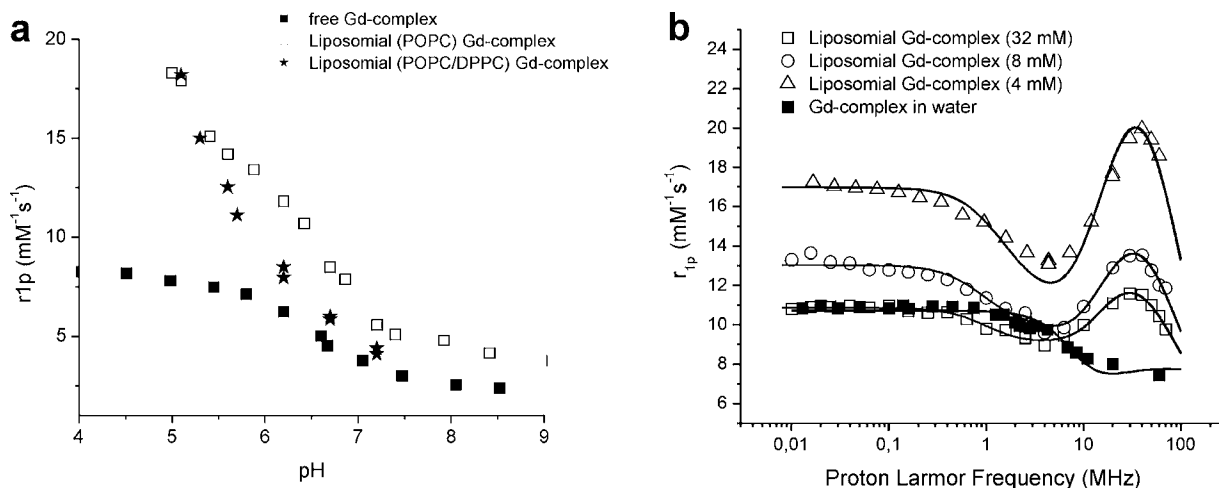


**Figure 2.** (a) Proton longitudinal relaxivity as a function of the pH measured at 25 °C and 20 MHz for free Gd-DO3Asa (■) and for liposomes including 4 mM Gd-DO3Asa [(□) –70% POPC, 25% Chol, and 5% PEG-2000-methoxy; (★) 35% POPC, 35% DPPC, 25% Chol, and 5% PEG-2000-methoxy]. The observed relaxation rates are normalized to 1 mM concentration of gadolinium(III). (b) Proton longitudinal relaxivity as a function of the applied magnetic field measured at 25 °C and pH 5 for free Gd-DO3Asa (■) and for liposomes (70% POPC, 25% Chol, 5% PEG-2000-methoxy) including 4 mM (Δ), 8 mM (○), and 32 mM (□) Gd-DO3Asa.

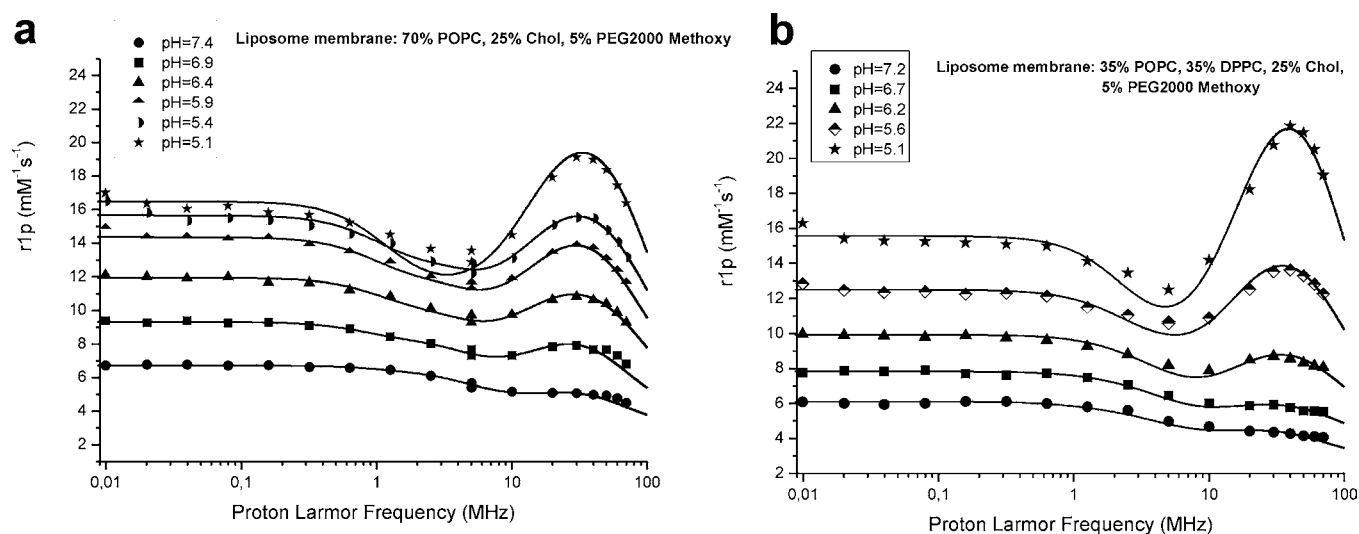


**Figure 3.** (a) Proton longitudinal relaxivity as a function of the applied magnetic field measured at 25 °C for liposomes (70% POPC, 25% Chol, 5% PEG-2000-methoxy) including 4 mM Gd-DO3Asa in different pH conditions in the range 5.1–7.4. (b) Proton longitudinal relaxivity as a function of the applied magnetic field measured at 25 °C for liposomes (35% POPC, 35% DPPC, 25% Chol, 5% PEG2000 Methoxy) including 4 mM Gd-DO3Asa in different pH conditions in the range 5.1–7.2. The observed relaxation rates are normalized to 1 mM concentration of gadolinium(III).

**Table 1. Principal Relaxometric Parameters Obtained from Fitting of the NMRD Profiles Reported in Figures 2 and 3**

		(A) Liposome Membrane Composition: 70% POPC, 25% Chol, and 5% PEG-2000-methoxy						
		liposomes						
		Gd-DO3Asa at pH 5	pH 5.1	pH 5.4	pH 5.9	pH 6.4	pH 6.9	pH 7.4
$\Delta^2 \times 10^{19} \text{ (s}^{-2}\text{)}$	cavity	2.30 ± 0.71	3.00 ± 0.52	2.05 ± 0.55	1.77 ± 0.48	1.58 ± 0.62	1.53 ± 0.63	2.21 ± 0.58
	membrane		1.54 ± 0.23	1.23 ± 0.11	1.17 ± 0.23	1.21 ± 0.31	1.01 ± 0.14	1.38 ± 0.24
$\tau_V \text{ (ps)}$	cavity	25.5 ± 1.8	28.6 ± 2.3	27.2 ± 1.8	25.0 ± 2.4	29.4 ± 2.8	30.1 ± 2.9	35.4 ± 3.1
	membrane		22.4 ± 1.8	23.9 ± 2.0	24.8 ± 1.9	25.4 ± 2.1	26.5 ± 2.5	25.7 ± 2.3
$\tau_R \text{ (ps)}$	cavity	94.0 ± 2.6	85.0 ± 1.6	95.0 ± 2.1	85.3 ± 3.1	84.6 ± 1.8	95.2 ± 2.2	95.0 ± 2.4
	membrane		3021 ± 32	3048 ± 18	3070 ± 22	2983 ± 24	3050 ± 32	3240 ± 48
$\tau_M \text{ (ns)}$	cavity	94.0 ± 2.1	94 <sup>a</sup>	94 <sup>a</sup>	94 <sup>a</sup>	94 <sup>a</sup>	94 <sup>a</sup>	94 <sup>a</sup>
	membrane		305 ± 15	293 ± 8.5	242 ± 10	300 ± 22	90 ± 6.2	90 ± 5.8
$q$	cavity	2 <sup>a</sup>	2 <sup>a</sup>	2 <sup>a</sup>	1.7 <sup>a</sup>	1.2 <sup>a</sup>	0.7 <sup>a</sup>	0.4 <sup>a</sup>
	membrane		1 <sup>a</sup>	0.7 <sup>a</sup>	0.6 <sup>a</sup>	0.5 <sup>a</sup>	0.25 <sup>a</sup>	0.15 <sup>a</sup>
$f$			0.7 ± 0.055	0.5 ± 0.032	0.4 ± 0.071	0.4 ± 0.060	0.3 ± 0.013	0.2 ± 0.012
$P_w \times 10^{-5} \text{ (cm s}^{-1}\text{)}$			140 ± 8.5	147 ± 10	150 ± 9.3	156 ± 8.6	148 ± 8.4	150 ± 7.3
		(B) Liposome Membrane Composition: 35% POPC, 35% DPPC, 25% Chol, and 5% PEG-2000-methoxy						
		liposomes						
		pH 5.1	pH 5.6	pH 6.2	pH 6.7	pH 7.2		
$\Delta^2 \times 10^{19} \text{ (s}^{-2}\text{)}$	cavity	2.97 ± 0.44	4.83 ± 0.32	4.00 ± 0.52	4.00 ± 0.27	3.05 ± 0.30		
	membrane	2.49 ± 0.51	1.97 ± 0.22	1.97 ± 0.31	1.64 ± 0.18	1.00 ± 0.12		
$\tau_V \text{ (ps)}$	cavity	18.2 ± 1.5	22.4 ± 2.3	19.6 ± 1.8	20.7 ± 2.1	19.4 ± 1.6		
	membrane	26.4 ± 2.3	29.4 ± 2.5	30.0 ± 1.8	29.8 ± 2.3	28.3 ± 1.9		
$\tau_R \text{ (ps)}$	cavity	93.5 ± 4.2	85.2 ± 3.1	85.6 ± 3.6	87.3 ± 2.8	95.0 ± 4.1		
	membrane	3037 ± 48	2988 ± 25	3150 ± 51	3012 ± 36	3028 ± 12		
$\tau_M \text{ (ns)}$	cavity	94.0 <sup>a</sup>	94.0 <sup>a</sup>	94.0 <sup>a</sup>	94.0 <sup>a</sup>	94.0 <sup>a</sup>		
	membrane	301 ± 10	315 ± 8.3	296 ± 12	306 ± 7.3	96.0 ± 4.5		
$q$	cavity	2 <sup>a</sup>	2 <sup>a</sup>	1.5 <sup>a</sup>	0.8 <sup>a</sup>	0.4 <sup>a</sup>		
	membrane	1 <sup>a</sup>	0.7 <sup>a</sup>	0.5 <sup>a</sup>	0.3 <sup>a</sup>	0.2 <sup>a</sup>		
$f$		0.7 ± 0.028	0.5 ± 0.022	0.3 ± 0.011	0.2 ± 0.015	0.1 ± 0.008		
$P_w \times 10^{-5} \text{ (cm s}^{-1}\text{)}$		146 ± 8.2	100 ± 3.4	70.0 ± 2.6	54.5 ± 1.8	30.0 ± 1.6		

<sup>a</sup>Fixed during the fitting procedure.

slowed upon intercalation of the gadolinium complex in the bilayer membrane.

Upon inspection of the data reported in Table 1, it comes out that, while some of the principal relaxometric parameters ( $\tau_R$ ,  $\tau_M$ ,  $\Delta^2$ , and  $\tau_V$ ) do not change in a significative way by changing the

pH of the liposomes' suspensions, on going from acidic to basic pH, there is a progressive reduction of the number of inner-sphere water molecules ( $q$ ) and a concomitant reduction of the fraction of intercalated gadolinium complexes over the encapsulated ones ( $f$ ). In the used model, the number of

**Table 2. Principal Relaxometric Parameters of the Different Gd-DO3Asa-Containing Systems Determined by NMRD Analysis of Data Reported in Figure 2b (pH 5, 25 °C)**

	aqueous Gd-DO3Asa	liposomal Gd-DO3Asa (4 mM)	liposomal Gd-DO3Asa I (8 mM)	liposomal Gd-DO3Asa (32 mM)
$r_{1p}$ (at 20 MHz; $\text{mM}^{-1} \text{s}^{-1}$ )	8.0	17.7	12.9	11.2
$\Delta^2 \times 10^{19}$ ( $\text{s}^{-2}$ )				
	cavity	2.30 $\pm$ 0.71	3.05 $\pm$ 0.52	7.41 $\pm$ 0.82
	membrane		1.54 $\pm$ 0.23	1.45 $\pm$ 0.16
$\tau_v$ (ps)				
	cavity	25.5 $\pm$ 1.8	28.6 $\pm$ 2.3	21.0 $\pm$ 0.8
	membrane		22.4 $\pm$ 1.8	19.8 $\pm$ 1.6
$\tau_R$ (ps)				
	cavity	94.0 $\pm$ 2.6	85.0 $\pm$ 3.6	80.4 $\pm$ 2.4
	membrane		3021 $\pm$ 32	3048 $\pm$ 12
$\tau_M$ (ns)				
	cavity	94.0 $\pm$ 2.1	94.0 <sup>a</sup>	94.0 <sup>a</sup>
	membrane		305 $\pm$ 15	286 $\pm$ 8.5
$q$				
	cavity	2 <sup>a</sup>	2 <sup>a</sup>	2 <sup>a</sup>
	membrane		1 <sup>a</sup>	1 <sup>a</sup>
$f$				
$P_w \times 10^{-5}$ ( $\text{cm s}^{-1}$ )		0.7 $\pm$ 0.080	0.4 $\pm$ 0.025	0.3 $\pm$ 0.014
		140 $\pm$ 8.5	100 $\pm$ 10	120 $\pm$ 6.4

<sup>a</sup>Fixed during the fitting procedure.

inner-sphere water molecules is not an output parameter, but it has to be fixed as an input constant. The best fitting of experimental data has been obtained by decreasing the  $q$  value as a function of increasing pH of the solutions.

Both  $q$  and  $f$  are responsible for the relaxivity decrease observed on going from pH 5 to 7. Moreover, in the case of formulation B (DPPC/POPC), also the liposome's permeability changes as a function of the pH. It is known that the use of saturated phospholipids (i.e., DPPC), in the vesicles formulation, reduces the permeability to water.<sup>13</sup> The progressive increase of intercalated Gd-DO3Asa complexes, obtained as a consequence of the medium acidification, causes an increase in the water permeability ( $P_w$ ) that, at pH 5, reaches a value that is very close to that of the highly permeable liposome A.

A similar effect was observed by Terreno et al. in a related work.<sup>14</sup>

Another important finding deals with the reduction of inner-sphere water molecules of the membrane-incorporated gadolinium complexes with respect to the encapsulated ones. In fact, at pH 5, for both liposome formulations, the best fitting of the NMRD profiles has been obtained by imposing only one inner-sphere water molecule for the membrane-incorporated species.

In summary, the observed decrease in relaxivity on going from acidic to basic pH appears to be ascribable to a complex interplay of three factors: (1) a change in the inner-sphere hydration of the gadolinium complex (lower hydration on going from pH 5 to 7.4); (2) a change in the intraliposomal distribution of the gadolinium complex (higher fraction of membrane-incorporated probe at acidic pH, which leads to a higher molecular reorientational time ( $\tau_R$ ) of the system); (3) in the case of POPC/DPPC-containing liposomes, a change in the vesicle membrane permeability to water ( $P_w$ ) caused by the different distributions of the gadolinium complex between the cavity and membrane as a function of the pH (higher water permeability at acidic pH).

Further support to the hypothesis of an acid-driven insertion of Gd-DO3Asa in the phospholipidic membrane was found in analysis of the NMRD profiles acquired on liposomes (formulation A) containing different concentrations of Gd-DO3Asa and normalized to the 1 mM concentration of gadolinium(III) (Figure 2b). Increasing the concentration of Gd-DO3Asa in the solution used for hydration of the lipidic film, the relaxivity decreases along the entire range of investigated

frequencies and particularly in the high-field region. This behavior may be accounted for in terms of a differential distribution of the gadolinium complex between the internal liposomal aqueous cavity and the phospholipidic membrane; i.e., the molar fraction of the "free" gadolinium complex is higher when its total concentration is higher. NMRD data were fitted according to the same model as that used for data reported in Figure 3.

For all of the liposomal formulations, the obtained relaxometric parameters relative to the encapsulated fraction of the gadolinium complex are similar to those determined for the free complex, whereas the parameters relative to the membrane-incorporated fraction are almost identical in all considered systems (see Table 2). The elongation in the  $\tau_R$  and  $\tau_M$  parameters, for the membrane-incorporated species, observed for the 4 mM formulation, was also confirmed when the concentration of the hydration solutions was brought to 8 and 32 mM. From the results of the fitting procedure, it appears that the membrane-incorporated gadolinium complexes lose one of the coordinated inner-sphere water molecules, giving a  $q = 1$  system also at acidic pH (pH 5).  $P_w$  values found for the three liposomes are in the range  $(100\text{--}140) \times 10^{-5} \text{ cm s}^{-1}$  of reported values for liposomes with similar membrane composition.<sup>14</sup> The consistent variation in the relaxivity values of liposomes loaded with 4, 8, and 32 mM Gd-DO3Asa may be then substantially ascribed to differences in the cavity–membrane distribution of the gadolinium complexes because the distribution factor  $f$  steadily decreases from 0.7 to 0.4 and 0.3 upon an increase in the concentration of the paramagnetic complex.

On the basis of these findings, one may envisage a process that, upon protonation of the sulfonamide moiety and the consequent removal of the arm from the coordination cage of the gadolinium(III) ion, prompts the lipophilic substituent to enter more deeply into the liposomal membrane. One may further speculate that this movement brings the Gd-DO3A moiety closer to the phosphate ester heads of the phospholipidic components of the liposomes membrane, which, upon entering the coordination cage of the gadolinium(III) ion, leads to the observed reduction (from  $q = 2$  to 1) of the number of inner-sphere water molecules. This process could also be responsible for the observed elongation of the exchange lifetime ( $\tau_M$ ) of the remaining water molecule, which, with the complex being inserted into the bilayer membrane, could be more hampered in

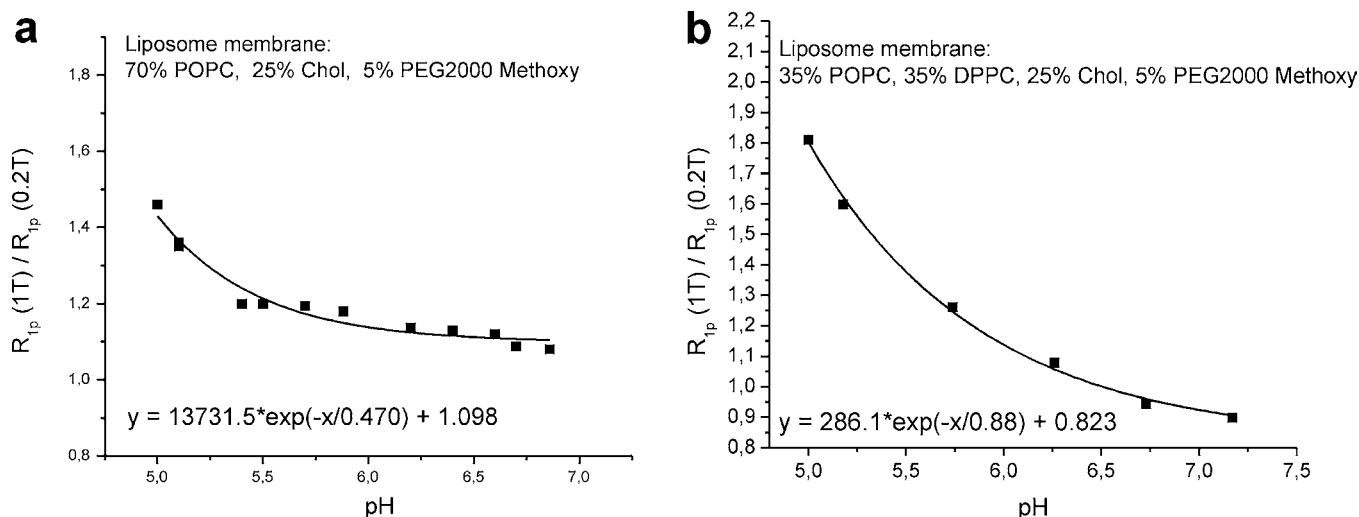


**Figure 4.** Exponential dependence of the ratio of observed relaxation rates at 1 and 0.2 T from the pH of solutions containing liposomes A (a) and B (b).

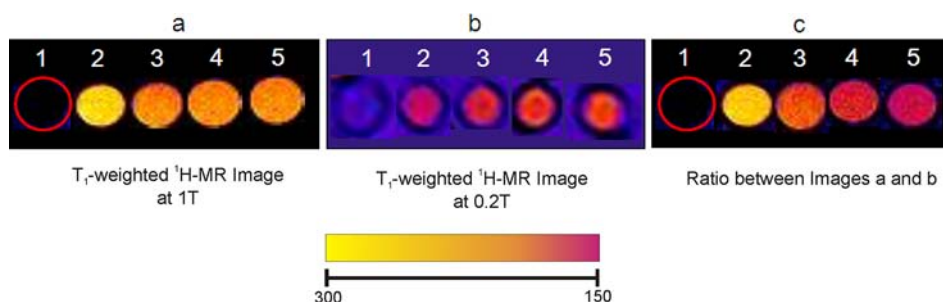


**Figure 5.** MR images of a phantom containing five different solutions as referred to in the text. (a)  $T_1$ -weighted spin-echo  $^1\text{H}$  MR image acquired at 1 T [TR/TE/NEX (150/18/10), FOV  $3 \times 3 \text{ cm}^2$ , 1 slice 2 mm]. (b)  $T_1$ -weighted spin-echo  $^1\text{H}$  MR image acquired at 0.2 T [TR/TE/NEX (150/18/30), FOV  $3 \times 3 \text{ cm}^2$ , 1 slice 5 mm]. (c)  $T_1$ -weighted spin-echo  $^1\text{H}$  MR image acquired at 1 T and divided for the signal intensities measured at 0.2 T. The color scale bar refers to the signal intensities.

its exchange with solvent water molecules. The Gd-DO3A chelate, and several of its derivatives, are, in fact, known to form ternary complexes with oxygen-donor ligands.<sup>1,15</sup>

**Setup of the Ratiometric Method for the Concentration-Independent MRI pH-Reporting System.** Through exploitation of the differences in the characteristic shapes of the NMRD profiles associated with suspensions of liposomes A and B as a function of the pH (Figure 3), it was deemed of interest to set up a ratiometric method to make their pH responsiveness independent from the concentration of the gadolinium complex. The ratio between the paramagnetic contribution to the observed relaxation rates (eqs 1 and 2) at two different magnetic fields [namely, 1 T (40 MHz) and 0.2 T (8.5 MHz)] is, in fact, independent of the concentration of the gadolinium probe (eq 3) but depends (with a monoexponential correlation) on the actual pH of the solution, as depicted in Figure 4.

$$R_{1p}(1\text{ T}) = R_{1\text{obs}}(1\text{ T}) - R_{1\text{id}} = r_{1p}(1\text{ T}) \times [\text{Gd}] \quad (1)$$

$$R_{1p}(0.2\text{ T}) = R_{1\text{obs}}(0.2\text{ T}) - R_{1\text{id}} = r_{1p}(0.2\text{ T}) \times [\text{Gd}] \quad (2)$$

$$R_{1p}(1\text{ T})/R_{1p}(0.2\text{ T}) = r_{1p}(1\text{ T})/r_{1p}(0.2\text{ T}) \quad (3)$$

By a decrease of the pH, the NMRD profiles of Gd-DO3A-loaded liposomes display a progressively higher relaxivity peak centered at 40 MHz, which, in turn, affects the value of the ratio reported in eq 3.

The proof of concept was acquired on a phantom consisting of five tubes containing suspensions of liposome (membrane formulation B, hydrated with 4 mM Gd-DO3A) at different dilutions and pH values. The phantom was imaged at 1 and 0.2 T.  $T_1$  relaxation rates of all the solutions were also measured by means of a standard inversion-recovery sequence. The phantom composition was as follows: (1) water; (2) gadolinium(III) total concentration = 0.063 mM, pH 5.50; (3) gadolinium(III) total concentration = 0.104 mM, pH 5.74; (4) gadolinium(III) total concentration = 0.190 mM, pH 6.7; (5) gadolinium(III) total concentration = 0.260 mM, pH 7.3.

When  $T_1$ -weighted  $^1\text{H}$  MR images at 1 and 0.2 T are acquired, the obtained signal intensities (Figure 5a,b) are not informative on the pH values of the solutions contained in the 2–5 capillaries. Conversely, upon division of the signal intensities of the image recorded at 1 T by the signal intensity values measured at 0.2 T, an image that restores the relationship between the signal intensity and pH values is obtained, as is shown in Figure 5c.

Finally, through the use of the relationship between the  $R_{1p}(1\text{ T})/R_{1p}(0.2\text{ T})$  and pH (Figure 4b), the MR imaging data may be analyzed to get an estimation of the pH of the five samples. Figure 6 shows a good correspondence between the pH measured by a pH electrode and the values determined by this ratiometric method (error ca. 3.5%).

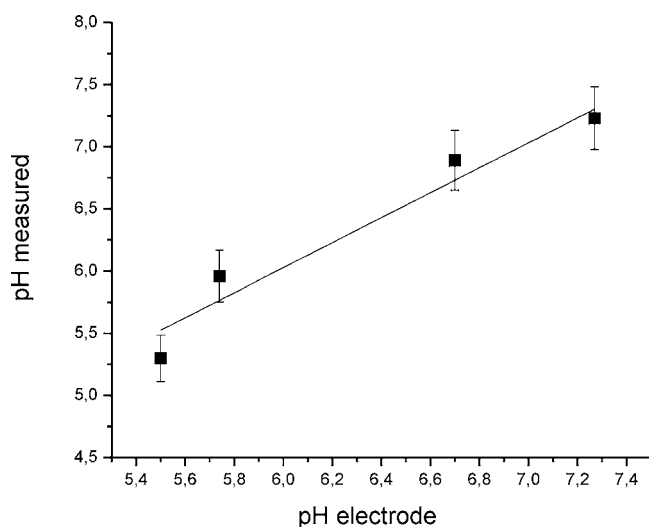


**Figure 6.** Linear relationship between the pH values measured through a pH electrode and through this ratiometric method. The linear correlation factor ( $R$ ) is 0.942, and the slope of the line is 1.004.

## CONCLUSION

The detailed relaxometric analysis of the NMRD profiles of Gd-DO3Asa-loaded liposome suspensions has allowed us to get an in-depth knowledge of the behavior of the amphiphilic, pH-responsive complex that distributes between the inner aqueous cavity and the liposomal membrane. It has been found that, upon protonation of the sulfonamide moiety, the neutral complex increases its affinity toward the lipophilic liposome's membrane and shifts more inside the phospholipid bilayer. This shift is accompanied by an increased water permeability across the liposomal membrane and a decreased hydration of the gadolinium(III) center. It is summarized that the latter effect may be accounted for in terms of the involvement of donor atoms from the phospholipid polar heads.

Importantly, Gd-DO3Asa-loaded liposomes maintain the pH responsiveness of the unbound paramagnetic complex, and their relaxivities are markedly affected by the magnetic field strength. This finding has prompted the setup of a ratiometric method for measurement of the pH based on a comparison of the relaxation effects at different magnetic fields. The proposed method adds to the available approaches to map the pH by MRI and offers an alternative tool for accessing measurement of the pH without prior knowledge of the concentration of the paramagnetic agent.

Moreover, the surface of the liposomes can be further functionalized to host vectors that endow the supramolecular adduct with targeting as well as multimodal capabilities for innovative applications in the field of medical diagnosis and imaging-guided therapies.

## ASSOCIATED CONTENT

### Supporting Information

Model used to analyze the relaxivity for the liposome-loaded gadolinium complexes, NMRD fitting, table of liposome membrane compositions, and figure of proton longitudinal relaxivity as a function of the applied magnetic field. This material is available free of charge via the Internet at <http://pubs.acs.org>.

## AUTHOR INFORMATION

### Corresponding Author

\*E-mail: [silvio.aime@unito.it](mailto:silvio.aime@unito.it). Fax: +390116706487. Tel: +390116706451.

### Notes

The authors declare no competing financial interest.

## ACKNOWLEDGMENTS

Economic and scientific support from Research Councils UK and the Engineering and Physical Sciences Research Council, under the Basic Technology scheme (FFC-MRI Project EP/E036775/1), Regione Piemonte (PIIMDMT and Nano-IGT projects), Cost Action TD1004 (Theranostics Imaging and Therapy: An Action to Develop Novel Nanosized Systems for Imaging-Guided Drug Delivery) are gratefully acknowledged. S.A. gratefully acknowledges the assignment of the Hans Fisher Seminar Fellowship from the Institute for Advanced Study, TUM (Munich, Germany).

## REFERENCES

- (1) Lowe, M. P.; Parker, D.; Reany, O.; Aime, S.; Botta, M.; Castellano, G.; Gianolio, E.; Pagliarin, R. *J. Am. Chem. Soc.* **2001**, *123*, 7601–7609.
- (2) Aime, S.; Botta, M.; Geninatti Crich, S.; Giovenzana, G. B.; Palmisano, G.; Sisti, M. *Chem. Commun.* **1999**, *16*, 1577–1578.
- (3) Zhang, S. R.; Wu, K. C.; Sherry, A. D. *Angew. Chem., Int. Ed.* **1999**, *38*, 3192–3194.
- (4) Gianolio, E.; Napolitano, R.; Fedeli, F.; Arena, F.; Aime, S. *Chem. Commun.* **2009**, *40*, 6044–6046.
- (5) Frullano, L.; Catana, C.; Benner, T.; Sherry, A. D.; Caravan, P. *Angew. Chem., Int. Ed.* **2010**, *49*, 2382–2384.
- (6) Gianolio, E.; Maciocco, L.; Imperio, D.; Giovenzana, G. B.; Simonelli, F.; Abbas, K.; Bisi, G.; Aime, S. *Chem. Commun.* **2011**, *47*, 1539–1541.
- (7) (a) Aime, S.; Barge, A.; Delli Castelli, D.; Fedeli, F.; Mortillaro, A.; Nielsen, F. U.; Terreno, E. *Magn. Reson. Med.* **2002**, *47*, 639–648. (b) Delli Castelli, D.; Terreno, E.; Aime, S. *Angew. Chem., Int. Ed.* **2011**, *50*, 1798–1800.
- (8) Gallagher, F. A.; Kettunen, M. I.; Brindle, K. M. *NMR Biomed.* **2011**, *24*, 1006–1015.
- (9) (a) Lokling, K. E.; Fossheim, S. L.; Skurtveit, R.; Bjornerud, A.; Klaveness, J. *Magn. Reson. Imaging* **2001**, *19*, 731–738. (b) Lokling, K. E.; Fossheim, S. L.; Klaveness, J.; Skurtveit, R. *J. Controlled Release* **2004**, *98*, 87–95. (c) Torres, E.; Mainini, F.; Napolitano, R.; Fedeli, F.; Cavalli, R.; Aime, S.; Terreno, E. *J. Controlled Release* **2011**, *154*, 196–202.
- (10) (a) Delli Castelli, D.; Gianolio, E.; Geninatti Crich, S.; Terreno, E.; Aime, S. *Coord. Chem. Rev.* **2008**, *252*, 2424–2443. (b) Accardo, A.; Tesaro, D.; Aloj, L.; Pedone, C.; Morelli, G. *Coord. Chem. Rev.* **2009**, *253*, 2193–2213. (c) Accardo, A.; Tesaro, D.; Morelli, G.; Gianolio, E.; Aime, S.; Vaccaro, M.; Mangiapia, G.; Paduano, L.; Schillen, K. *J. Biol. Inorg. Chem.* **2007**, *12*, 267–276. (d) Hak, S.; Sanders, H. M. H. F.; Agrawal, P.; Langereis, S.; Grull, H.; Keizer, H. M.; Arena, F.; Terreno, E.; Strijkers, G. J.; Nicolay, K. *Eur. J. Pharm. Biopharm.* **2009**, *72*, 397–404.
- (11) (a) Solomon, I. *Phys. Rev.* **1955**, *99*, 559. (b) Bloembergen, N. *J. Chem. Phys.* **1957**, *27*, 572. (c) Bloembergen, N.; Morgan, L. O. *J. Chem. Phys.* **1961**, *34*, 842.
- (12) (a) Nicolle, G. M.; Toth, E.; Eisenwiener, K. P.; Macke, H. R.; Merbach, A. E. *J. Biol. Inorg. Chem.* **2002**, *7*, 757–769. (b) Torres, S.; Martins, J. A.; Andr e, J. P.; Geraldes, C. F. G. C.; Merbach, A. E.; Toth, E. *Chem.—Eur. J.* **2006**, *12*, 940–948.
- (13) (a) Koenig, S. H.; Ahkong, Q. F.; Brown, R. D.; Lafleur, M.; Spiller, M.; Unger, E.; Tilcock, C. *Magn. Reson. Med.* **1992**, *23*, 275–286. (b) Huster, D.; Jin, A. J.; Arnold, K.; Gawrisch, K. *Biophys. J.* **1997**, *73*, 855–864.

(14) Terreno, E.; Sanino, A.; Carrera, C.; Delli Castelli, D.; Giovenzana, G. B.; Lombardi, A.; Mazzon, V.; Milone, L.; Visigalli, M.; Aime, S. *J. Inorg. Biochem.* **2008**, *102*, 1112–1119.

(15) (a) Terreno, E.; Botta, M.; Boniforte, P.; Bracco, C.; Milone, L.; Mondino, B.; Uggeri, F.; Aime, S. *Chem.—Eur. J.* **2005**, *11*, 5531–5537.

(b) Aime, S.; Gianolio, E.; Terreno, E.; Giovenzana, G. B.; Pagliarin, R.; Sisti, M.; Palmisano, G.; Botta, M.; Lowe, M. P.; Parker, D. *J. Biol. Inorg. Chem.* **2000**, *5*, 488–497. (c) Digilio, G.; Menchise, V.; Gianolio, E.; Catanzaro, V.; Carrera, C.; Napolitano, R.; Fedeli, F.; Aime, S. *J. Med. Chem.* **2010**, *53*, 4877–4890.